Heliyon 6 (2020) e05278

Contents lists available at ScienceDirect

Heliyon

journal homepage: www.cell.com/heliyon

Research article

Computer-aided drug design against spike glycoprotein of SARS-CoV-2 to aid COVID-19 treatment

Muhammad Shehroz [a], Tahreem Zaheer [b], Tanveer Hussain [c,*]

[a] Department of Biotechnology, Virtual University of Pakistan, Peshawar, Pakistan
[b] Atta ur Rahman School of Applied Biosciences (ASAB), National University of Sciences and Technology (NUST), Islamabad, Pakistan
[c] Department of Molecular Biology, Virtual University of Pakistan, Lahore, Pakistan

ARTICLE INFO

Keywords:
Bioinformatics
Immunology
Virology
Computer-aided drug design
Drug binding
Infectious disease
Viral protein
Viruses
SARS-CoV-2
Receptor binding domain
Virtual screening
Lead compounds
Anti-Viral drugs
COVID-19

ABSTRACT

Background: SARS-CoV-2 has the Spike glycoprotein (S) which is crucial in attachment with host receptor and cell entry leading to COVID-19 infection. The current study was conducted to explore drugs against Receptor Binding Domain (RBD) of SARS-CoV-2 using *in silico* pharmacophore modelling and virtual screening approach to combat COVID-19.
Methods: All the available sequences of RBD in NCBI were retrieved and multiple aligned to get insight into its diversity. The 3D structure of RBD was modelled and the conserved region was used as a template to design pharmacophore using LigandScout. Lead compounds were screened using Cambridge, Drugbank, ZINC and TIMBLE databases and these identified lead compounds were screened for their toxicity and Lipinski's rule of five. Molecular docking of shortlisted lead compounds was performed using AutoDock Vina and interacting residues were visualized.
Results: Active residues of Receptor Binding Motif (RBM) in S, involved in interaction with receptor, were found to be conserved in all 483 sequences. Using this RBM motif as a pharmacophore a total of 1327 lead compounds were predicted initially from all databases, however, only eight molecules fit the criteria for safe oral drugs. Conclusion: The RBM region of S interacts with Angiotensin Converting Enzyme 2 (ACE2) receptor and Glucose Regulated Protein 78 (GRP78) to mediate viral entry. Based on *in silico* analysis, the lead compounds scrutinized herewith interact with S, hence, can prevent its internalization in cell using ACE2 and GRP78 receptor.
The compounds predicted in this study are based on rigorous computational analysis and the evaluation of predicted lead compounds can be promising in experimental studies.

1. Introduction

An epidemic started in December 2019 from Wuhan, China, where infected people suffered from pneumonia-like symptoms which later spread over more than 200 countries world-wide. The root cause of infection was found to be a novel virus that bore structural similarities with Severe Acute Respiratory Syndrome related Coronaviruses, hence named as SARS-CoV-2 (Bogoch et al., 2020; Hui et al., 2020; Paules et al., 2020; Tang et al., 2020). It's the seventh Coronavirus that has been isolated from humans and the third one to cause a severe infection leading to a global pandemic (Munster et al., 2020). The virus causes contagious disease which is termed as coronavirus disease 2019 (COVID-19) by WHO. The virus can be spread through common means such as air droplets and personal contacts etc. By the first week of January 2020, a total 4 cases were found to be positive with 7 critically ill and one death. But the number increased at a logarithmic scale making it an uncontrolled pandemic. Presently, more than 2 million positive cases are reported globally with more than 0.12 million deaths (Zhao et al., 2020). Middle East Respiratory Syndrome (MERS) and SARS-CoV are notorious for their fatality rates and have caused 36% and 10% deaths, respectively. However, despite belonging to same family, currently SARS-CoV-2 has a fatality rate of 2% but it is prone to vary in future (Baez-Santos et al., 2014; Organization, 2019; Udwadia and Raju, 2020; WHO, 2018; Widagdo et al., 2017).

SARS-CoV-2 is a single-stranded RNA virus having a genome size of approximately 30,000 bps. The Open Reading Frame (ORF) constitutes two types of proteins, structural (Spike (S) glycoprotein, small Envelope (E) glycoprotein and membrane (M) glycoprotein and nucleocapsid (N) protein) as well nonstructural (NS) protein (i.e. nsp1-16) (Ibrahim et al., 2019). Although all proteins of SARS-CoV-2 have an important role in pathogenesis

* Corresponding author.
E-mail address: tanveer.hussain@vu.edu.pk (T. Hussain).

https://doi.org/10.1016/j.heliyon.2020.e05278
Received 30 April 2020; Received in revised form 26 May 2020; Accepted 13 October 2020
2405-8440/© 2020 Published by Elsevier Ltd. This is an open access article under the CC BY-NC-ND license (http://creativecommons.org/licenses/by-nc-nd/4.0/).

and replication, S is a promising drug target as it is involved in attachment to the human cell and intracellular entry. It is a homo-trimeric protein that attaches itself to human angiotensin-converting enzyme 2 (ACE2) using its receptor-binding domain and mediates cell entry. The structure of S cleaves at the boundary between its two domains, i.e., S1 and S2. In the prefusion conformation, these subunits remain non-covalently attached. S2 subunit of protein encompasses the fusion machinery while S1 has a crucial role in attachment to the receptor as it contains the receptor binding domain (RBD) (Belouzard et al., 2012; Li et al., 2005a; Walls et al., 2020).

Moreover, Binding immunoglobulin Protein (BiP) also known as Glucose Regulating Protein 78 (GRP78) of humans is the master chaperon protein found on the lumen of the Endoplasmic Reticulum (ER) also has a role in viral recognition. This Chaperon protien bond to three enzymes Activating Transcription Factor 6 (ATF6), Inositol-Requiring Enzyme 1 (IRE1) and Protein kinase RNA-like Endoplasmic Reticulum Kinase (PERK) and release them after the accumulation of unfolded proteins (Lee, 2005; Li and Lee, 2006; Quinones et al., 2008; Rao et al., 2004). SARS-CoV-2 infection inhibits protein synthesis and enhance the process of protein refolding. It also brings the cell in a state of stress causing GRP78 to translocate to the cell membrane and expose its Substrate binding Domain (SBD) for virus recognition (Kim et al., 2006; Shen et al., 2002).

Researchers all around the world are endeavoring to find antiviral treatment to cater COVID-19. Several drugs like Favipiravir, Remdesivir, Arbidol, and Chloroquine are under investigational as well as clinical trials to treat it. Arbidol, Ribavirin, Chloroquine phosphate, Lopinavir/Ritonavir, and Immunity-boosting Interferon α (IFN-α) have also been included in the updated guidelines as therapy for COVID-19 by National Health Commission (NHC) of China. However, so far, no drug has been approved by Food and Drug Administration (FDA) (Dong et al., 2020). Computer-aided drug design project saves the cost and labor to test all the compounds in the lab and help in the screening of potent ligands/inhibitor that can target the majority of strains (Kapetanovic, 2008). Hence, the current study is aimed to explore drugs against S of SARS-CoV-2 using *in silico* pharmacophore modelling approach and virtual screening of lead compounds.

2. Materials and methods

2.1. Phylogenetic analysis of SARS-CoV-2 receptor binding domain (RBD)

Sequences of all available SARS-CoV-2 RBD in S were retrieved from NCBI. The detail of these sequences is mentioned in Supplementary file 1. These sequences also included reference SARS-CoV-2 and sequences of S reported from Pakistan. All these sequences were multiple aligned using CLUSTAL W in MegaX to get insight into the diversity of RBD region (Kumar et al., 2018). Moreover, a phylogenetic tree using Neighbour Joining method was constructed in MegaX in which evolutionary distances were computed using Poisson correction method (Kumar et al., 2018). The tree was labelled and visualized using iTOL (Letunic and Bork, 2019).

2.2. Structure prediction

The tertiary structure of SARS-CoV-2 was predicted using I-TASSER (Iterative Threading ASSEmbly Refinement) which assesses functionality and structural analysis of proteins (Yang and Zhang, 2015). The quality check of the modelled protein was performed as per the C score. C-score ranges from -5 to 2; a greater C-score suggests a better-refined model. The structure was modelled using S of the reference sequence (YP_009724390).

2.3. Binding pocket

The S of SARS-CoV-2 attaches the virus to ACE2 using defined RBD (LYS356-ASN536) on Spike which facilitates this interaction (Ibrahim et al., 2020). The Receptor Binding Motif (RBM) exhibits a concave like binding groove that binds to ACE2 and GRP78 (Li, 2016). The RBM region interacting with ACE2 and GRP78 was found to be between 473-489 amino acids (Ibrahim et al., 2020; Li et al., 2005b). These residues from binding pocket were used for designing pharmacophore.

2.4. Pharmacophore model generation

Virtual screening of drug from substantial libraries of compound is a popular method used in computer-aided drug design studies (Lyne, 2002). It is also regarded as a computational alternative of laborious experimental screening by employing high-throughput screening (HTS) (Stahura and Bajorath, 2012). One of the similar approaches is pharmacophore model-based screening that uses complex structural features of proteins for predicting interaction against library of lead compounds. In this study, LigandScout 4.3 was used to generate structure-based pharmacophore was designed based on active site residues of RBM in S and were also found to be conserved within SARS-CoV-2 (Wolber and Langer, 2005). The designed pharmacophore model was checked for all crucial chemical features.

2.5. Virtual screening of databases

Pharmacophore-based virtual screening of compounds repository was performed using Cambridge Structural Database (615923), ZINC database (133077), DrugBank (8706) and TIMBAL database (7207) containing distinct small molecules of molecular weight <1.2 kDa. These molecules that have potential to interact and mediate protein-ligand interactions were screened as lead compounds against shared features of pharmacophore (Groom et al., 2016; Higueruelo et al., 2013; Irwin and Shoichet, 2005; Wishart, 2012). A single library in LigandScout having ligand from all the databases was created and all ligand atoms were set free to move in the binding pocket. However, only lead interacting compounds were further examined for added parameters such as Lipinski's rule of five. The rule states that all the drugs shortlisted should have a molecular mass of <500 Da, no more than 5 Hydrogen Bond donors (HBD), less than 10 Hydrogen Bond Acceptors (HBA), and lastly should have octanol-water partition coefficient LogP under 5 (Kapetanovic, 2008).

2.6. Molecular docking and analysis of interacting residues

Molecular docking analyses of shortlisted lead compounds were performed using AutoDock Vina (Trott and Olson, 2009). The RBD region of S was protonated and grid scoring function was set to maximum, i.e. 1 Å. The grid box was placed at 79.461x, 167.644y, and 165.862z with a size of 16, 24, and 32. The interaction affinity as a scoring function was analyzed by docking lead compounds with RBM, sequentially. Docked complexes were visualized in UCSF Chimera using "view dock" function (Pettersen et al., 2004) and interacting residues were analyzed using Discovery studio Visualizer (2005).

3. Results and discussion

The coronavirus epidemic has caused an alarming situation throughout the world. The key to overcoming this infection is to understand the mechanism by which the virus interacts with the host receptor and predict effective treatment option to block this interaction. The S of SARS-CoV-2 contains a crucial domain involved in the attachment of the virus to host cell. Among 83 sequences, majority of the sequences belonged to China and USA. Among all sequence, 473 sequences were 100% conserved while remaining branched into separate nodes which further diverged (as can be seen in Figure 1).

The RBM region, YQAGSTPCNGVEGFNCY, in S is of prime importance as it encompasses the binding grove which is involved in attachment with ACE2 and GRP78. The active site residues present in this region were found to be conserved in 483 globally reported sequences

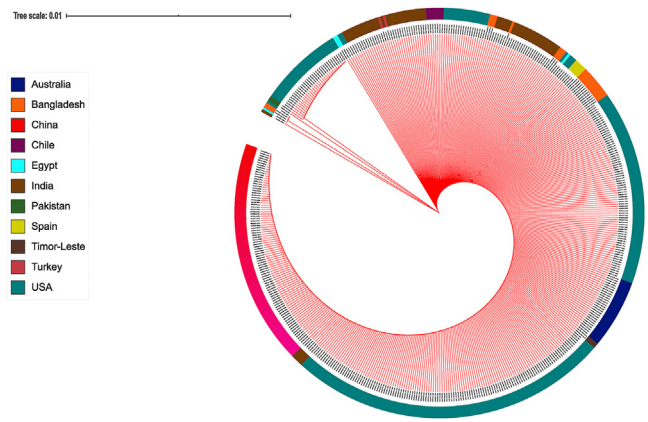

Figure 1. Phylogenetic analysis of RBD region of SARS-CoV-2. The outer color strip ring indicates the diversity of RBD region across the globe.

used in this study. The pharmacophore was designed based on this region and hence can give a global representation of SARS-CoV-2 RBM region. The antivirals reported herewith interact with RBM region of SARS-CoV-2 hence preventing its interaction with host cell receptors and can ward off COVID-19 (Hoffmann et al., 2020) (Ibrahim et al., 2020; Prajapat et al., 2020; Shang et al., 2020).

3.1. Structural properties of surface glycoprotein and RBD

The tertiary structure of S had a high confidence score i.e. 1.52 with a TM score of 0.825 and coverage of 0.82. The modelled structure showed 80% similarity with PDB ID 6nb6. The tertiary structure can be seen in Figure 2A.

The crucial domain from RBD involves in interaction with receptor ACE2 and GRP78 uses residues from 331-524. The structure of this region is shown in Figure 2B. The detailed secondary structure analysis of this domain shows that it has 1 antiparallel beta-sheet having no barrel, 1 beta-hairpin of class 68:70, 1 antiparallel classic beta bulge between (Residue X, Glu516A) (Residue 1, Thr393A), (Residue 3, Asn394A). It has 5 strands and 5 helices. Moreover, the structure also encompasses a total of 33 beta turns of type I, IV and VIII, 17 gamma turns (both inverse and classic) and 4 disulfide bonds (Figure 2 C). A detailed insight into the structure has been provided in Supplementary file 2.

3.2. Pharmacophore modelling

Pharmacophore based modelling and virtual screening to identify lead compounds is a popular method for *in silico* identification of drugs (Yang, 2010). All four databases used in this study are essential for computer-aided drug design projects. Several studies involving drugs in investigational studies, medicinal compounds from extracts and FDA approved drugs are present in the repository (Sudha et al., 2008). Computer-aided drug design predicts effective lead compounds without the investment of many resources (Kapetanovic, 2008). The pharmacophore was designed against the RBM region 473–489 amino acid position. The designed pharmacophore was screened against all the ligand present in databases to identify molecules having perfect bond order, hybridization state and chemical functionality. A total of 1327 hits were found based on the pharmacophore features against 764913 ligand molecules form all four databases. Among 1327 only 10 ligand molecules had a fit score of more than 50. Out of these 10, only 8 ligand molecules surpassed screening criteria and are reported here as effective inhibitors against the S of SARS-CoV-2. All the eight ligand molecules follow Lipinski rules of five and can be termed as safe oral drugs (Lipinski, 2004).The rule is also known as Rule of 5 or Pfizer's rule of five that specifically determine the druggable properties of a particular chemical compound to make it a safe orally active drug for humans. All the drugs shortlisted have molecular mass of <500 Da, no more than 5 HBD, no

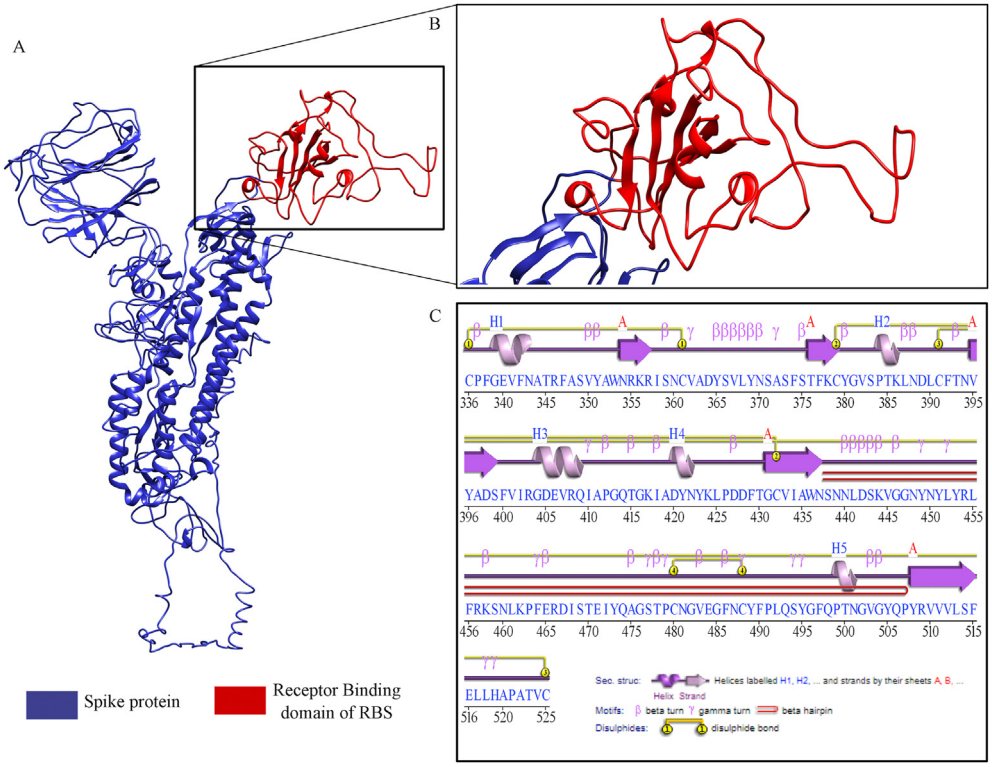

Figure 2. Tertiary structure of Spike glycoprotein and its receptor binding domain. A) The overall 3D structure of trimeric spike glycoprotein. B) Receptor binding domain (RBD) of Spike glycoprotein that interacts with ACE2 and GRP78. C) Secondary Structure of RBD containing information about helices, beta sheets and in-depth analysis of motifs present in RBD.

Table 1. Lead compounds having >50 fit score by virtual screening of pharmacophore against 764913 ligand molecules.

Lead Compound	Inhibitor	Pharmacophore Fit Score	Docking Score	Druggable Properties	Structure	Source
1	N-ethyl-2,3-difluoro-N-[(3R*,4R*)-3-hydroxy-1-(2-thienylcarbonyl)-4-piperidinyl]benzamide	57.94	-5.2	Toxic = NO Weight = 394.44 g/mol LogP = 2.76 HBD = 3 HBA = 1		Cambridge Database
2	7-acetyl-N-hexyl-2-pyridin-3-yl-5,6,7,8-tetrahydropyrido[3,4-d]pyrimidin-4-amine	57.72	-5.2	Toxic = NO Weight = 353.47 g/mol LogP = 3.70 HBD = 1 HBA = 4	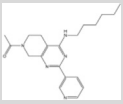	Cambridge Database
3	N-{3-[({1-[3-(4-fluorophenyl)-1,2,4-oxadiazol-5-yl]ethyl}carbamoyl)amino]-4-methylphenyl}acetamide	57.71	-5.3	Toxic = NO Weight = 401.44 g/mol LogP = 2.95 HBD = 4 HBA = 3	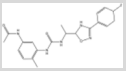	ZINC Database
4	6-(1H-imidazol-1-yl)-N-[1-(3,4,5-trifluorophenyl)ethyl]pyrimidin-4-amine	57.13	-5.2	Toxic = NO Weight = 323.32 g/mol LogP = 2.53 HBD = 2 HBA = 2	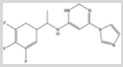	ZINC Database
5	7-acetyl-N-(3-phenylpropyl)-2-pyridin-3-yl-5,6,7,8-tetrahydropyrido[3,4-d]pyrimidin-4-amine	57.1	-4.9	Toxic = NO Weight = 387.49 g/mol LogP = 3.75 HBD = 1 HBA = 4	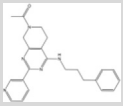	Cambridge Database
6	N-[2-(4-methyl-6,7-dihydro-5H-cyclopenta[d]pyrimidin-2-yl)ethyl]-N'-[3-(1,3-oxazol-5-yl)phenyl]urea	57.08	-4.8	Toxic = NO Weight = 363.42 g/mol LogP = 3.29 HBD = 2 HBA = 4	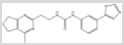	Cambridge Database
7	N-(isoxazol-3-ylmethyl)-N'-[4-methyl-3-(2-oxopyrrolidin-1-yl)phenyl]urea	57.06	-5.1	Toxic = NO Weight = 314.34 g/mol LogP = 2.70 HBD = 2 HBA = 3	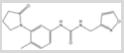	Cambridge Database
8	N-[4-methyl-3-(2-oxopyrrolidin-1-yl)phenyl]-N'-(tetrahydro-2H-pyran-4-ylmethyl)urea	57.06	-5.1	Toxic = NO Weight = 331.42 g/mol LogP = 2.67 HBD = 2 HBA = 3	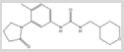	Cambridge Database

more than 10 HBA, and LogP value was also under 5. No inhibitor from TIMBLE database had a fit score of >50 so the lead compounds reported here are only from Cambridge and ZINC database (Table 1).

3.3. Molecular docking and analysis of interacting residues

These lead compounds, when docked against the RBD motif of S, showed significant interaction the binding affinity, also known as the Docking score of AutoDock vina is mentioned in column 4 of Table 1. The scoring power of AutoDock is reported to be the best among ten available docking programs in a study reported by Wag et al. (Wang et al., 2016).

The docking pose of all the lead compounds showed that they were interacting with the RBM motif in a confirmation that fits them in the binding pocket of RBM. The docking pose along with the list of interacting residues are illustrated in Figures 3, 4, 5, 6, 7, 8, 9, and 10. The interacting residues predicted in this study coincide with the binding residues reported in the literature. These residues are crucial in the interaction of S with ACE2 receptor and GRP78. These residues are GLY 476, THR 478, PRO 479, CYS 480, ASN 481, GLY 485, PHE 486, and CYS 488 for lead compound 1 as illustrated in Figure 3. The pharmacophore designed using RBM is highlighted in Figure 3A, while Figure 3B shows the two-dimensional structure of this lead compound also illustrating its HBA and HBD atoms. The lead compound 1 interacts with RBD with a docking score of -5.2. The lead compounds fit well in the pocket of RBM that is involved in attachment with host receptors. CYS 488 of RBM makes a pi Sulphur bond with an atom of lead compound 1. Residue ASN 481 makes a conventional hydrogen bond with the structure of lead compound 1 while pi alkyl bond is formed between the residue GLY 485 and lead compound 1 (Figure 3).

The lead compound 2 has 1 Hydrogen bond donor, 3 Hydrogen Bond Acceptor. The structure of pharmacophore is illustrated in Figures 4A, 4B and 4C. It is predicted to have one hydrophobic interact ion. It interacts with RBD with a docking score of -5.2. The interacting residues in case of lead compound 2 are GLY 476, THR 478, PRO 479, CYS 480, ASN 481, GLY 485, PHE 486, ASN 487, CYS 488 as illustrated in Figure 4 D,E, and F. S in complex with lead compound 2 also orients itself in a conformation that fits lead compound 2 in its binding pocket. It is noteworthy to mention that the residues involved in the interaction of lead compound 2 are the same as predicted for lead compound 1. GLY476, PRO479, CYS 480, GLY 485, PHE 486, ASN 487 residues are interacting with lead compounds 2 by Van der Waal interaction. ASN 481 makes conventional hydrogen bond while THR 478 interacts making pi hydrogen bond with lead compound 2 (as seen in Figure 4F).

The binding score of lead compound 3 is -5.3 that shows this lead compound shows the strongest interaction (in terms of docking score) with RBD of S. The interacting residues in this case are GLY 476, THR 478, CYS 480, ASN 481, GLY 482, VAL 483, GLU 484, GLY 485, PHE 486, ASN 487, and CYS 488 involved in the interaction with RBM of S. GLU 484, GLY 482, GLY 485, THR 478, ASN 487 interacts with lead compound 3 using Van der Waal's interaction. ASN 481, GLY 476 makes

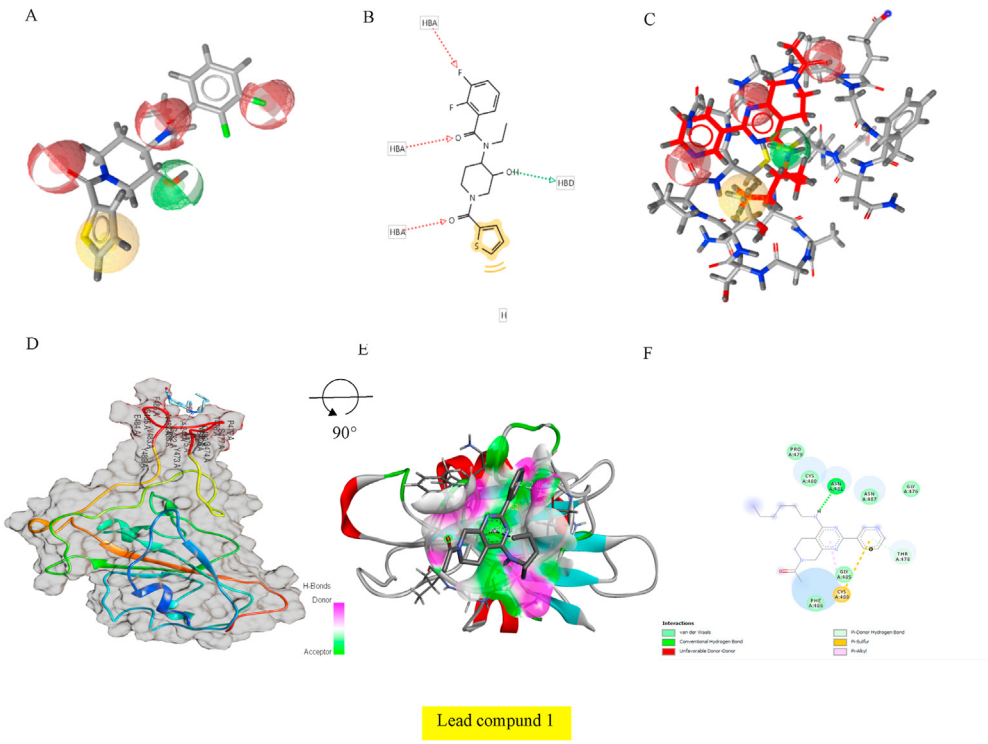

Figure 3. Virtually screened pharmacophore, lead molecule 1 and its interaction with RBD of spike glycoprotein. A) lead molecule 1 predicted in pharmacophore region B) 2D structure of lead compound with pharmacophore features C) 3D structure of lead compound within RBD D) lead compound docked in the binding groove of RBD E) vertical representation of lead compound interacting with RBM within RBD region F) 2D representation of interacting residues interacting with lead compound showing nature of interactions.

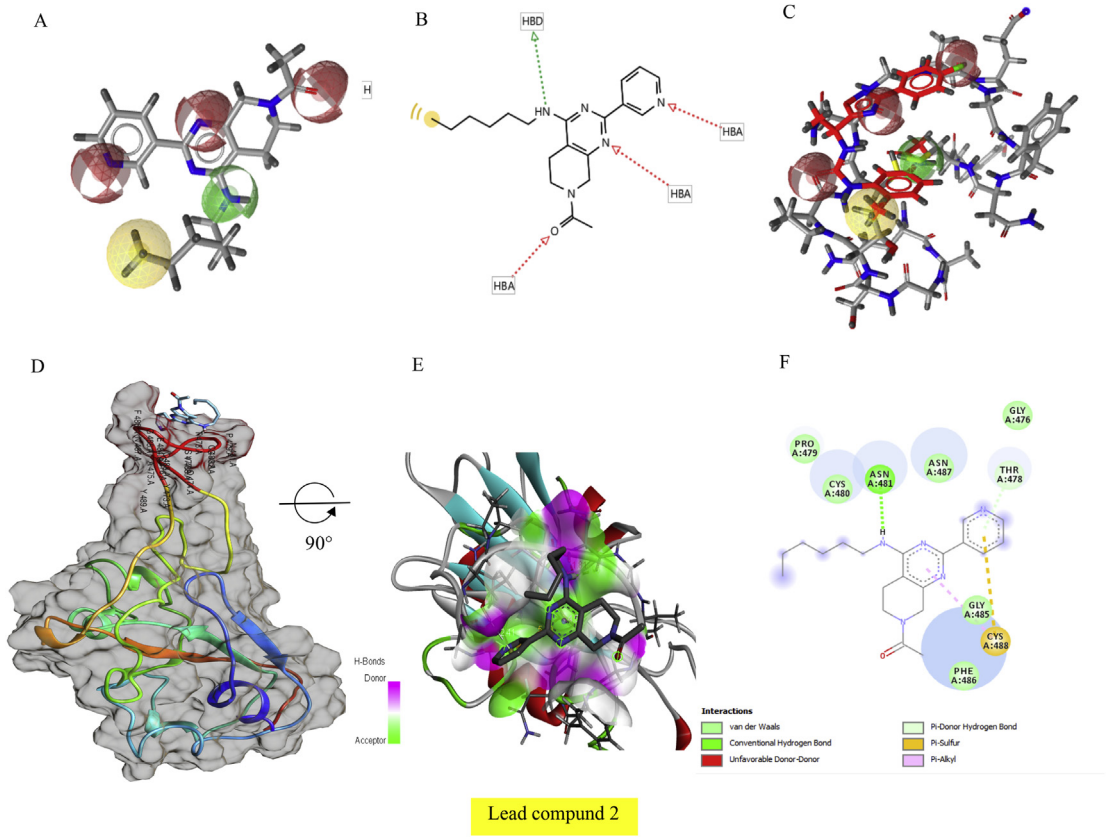

Figure 4. Virtually screened pharmacophore, lead molecule 2 and its interaction with RBD of spike glycoprotein. A) lead molecule 2 predicted in pharmacophore region B) 2D structure of lead compound with pharmacophore features C) 3D structure of lead compound within RBD D) lead compound docked in the binding groove of RBD E) vertical representation of lead compound interacting with RBM within RBD region F) 2D representation of interacting residues interacting with lead compound showing nature of interactions.

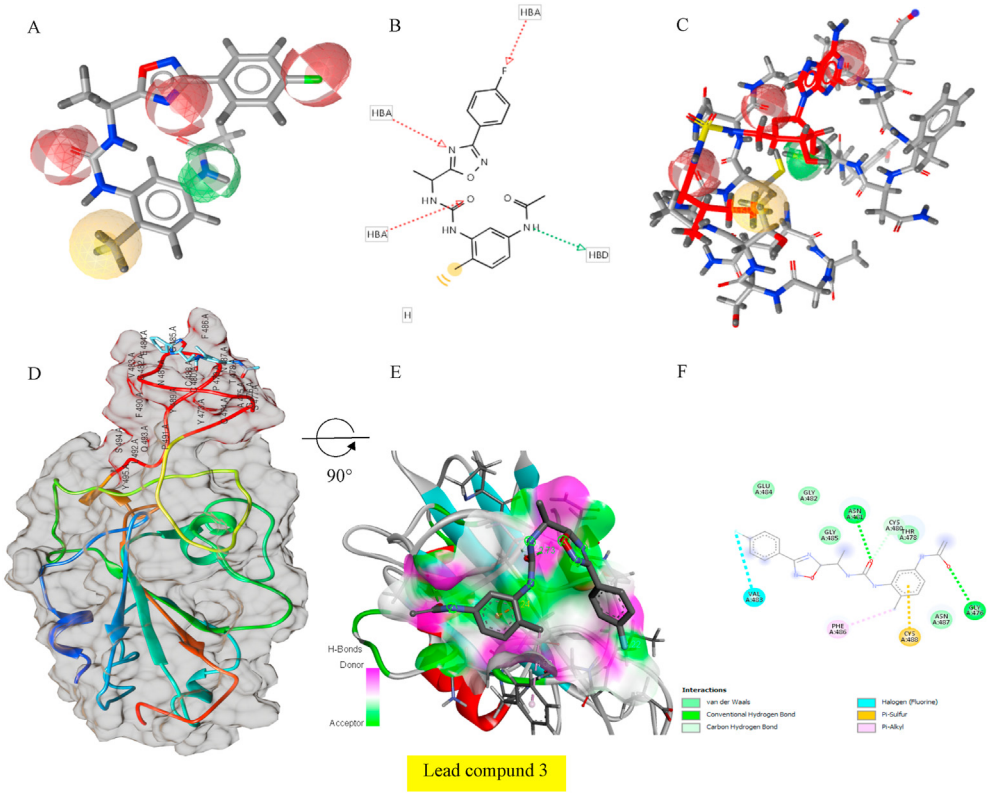

Figure 5. Virtually screened pharmacophore, lead molecule 3 and its interaction with RBD of spike glycoprotein. A) lead molecule 3 predicted in pharmacophore region B) 2D structure of lead compound with pharmacophore features C) 3D structure of lead compound within RBD D) lead compound docked in the binding groove of RBD E) vertical representation of lead compound interacting with RBM within RBD region F) 2D representation of interacting residues interacting with lead compound showing nature of interactions.

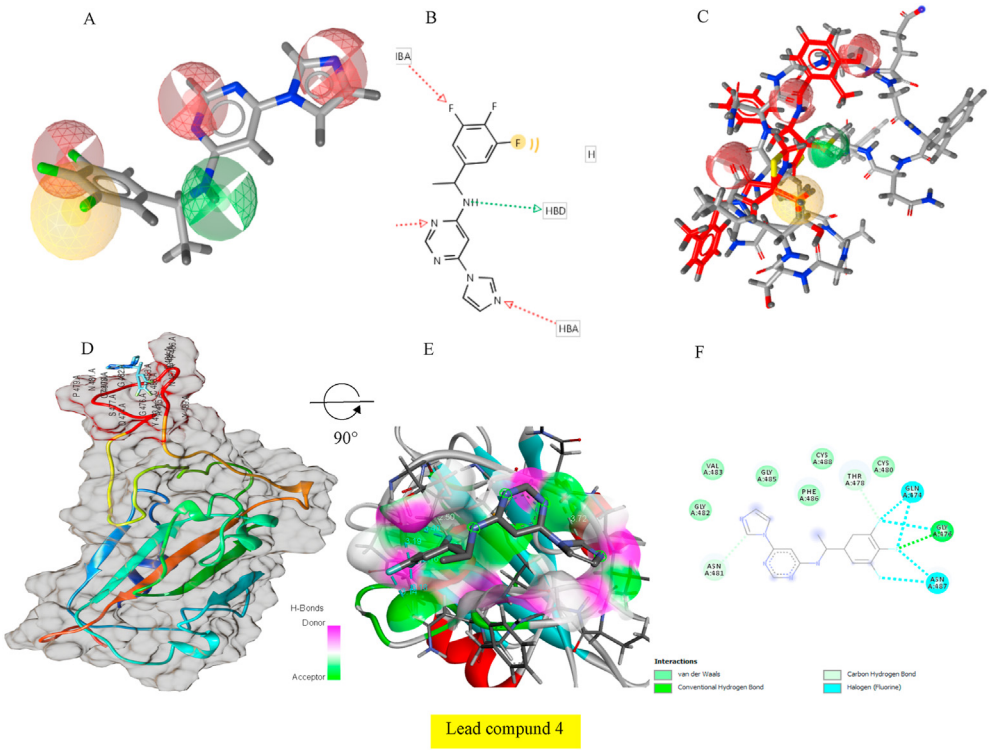

Figure 6. Virtually screened pharmacophore, lead molecule 4 and its interaction with RBD of spike glycoprotein. A) lead molecule 4 predicted in pharmacophore region B) 2D structure of lead compound with pharmacophore features C) 3D structure of lead compound within RBD D) lead compound docked in the binding groove of RBD E) vertical representation of lead compound interacting with RBM within RBD region F) 2D representation of interacting residues interacting with lead compound showing nature of interactions.

conventional hydrogen bond with lead compound. CYS 480 interacts by making C–H Hydrogen bond while VAL 483 interact using hydrogen bond. Lastly, PHE 486 and CYS 488 make pi alkyl and pi Sulphur bond, respectively (Figure 5).

The docking score of lead compound 4 is -5.2 (same as lead compound 1 and 2). The residues involved in the interaction of lead compound 4 are ASN 481, GLY482, VAL 483, GLY485, PHE486, CYS 488, THR 478, CYS 480, GLN 474, GLY 476, ASN 487. Among these residues, GLY 482, VAL 483, GLY 485, PHE 486, CYS 488, CYS 480 interact with lead compound 4 with Van der Waal's interaction. GLY 476 makes one conventional hydrogen bond, while 2 C–H hydrogen bonds are made by ASN 481 and

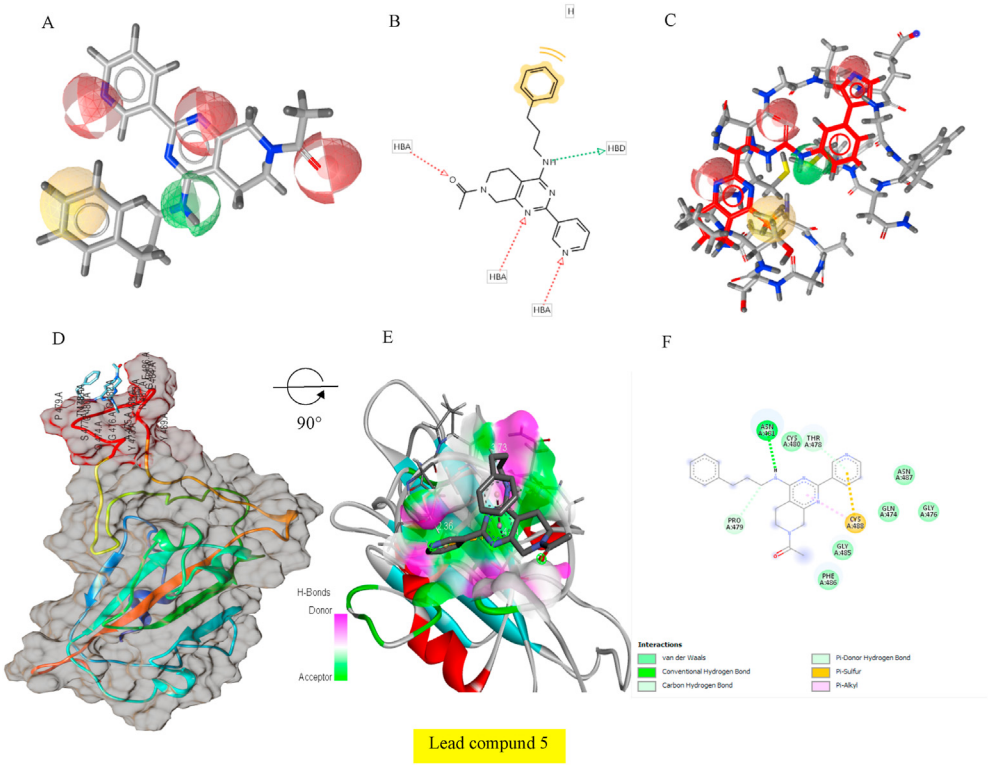

Figure 7. Virtually screened pharmacophore, lead molecule 5 and its interaction with RBD of spike glycoprotein. A) lead molecule 5 predicted in pharmacophore region B) 2D structure of lead compound with pharmacophore features C) 3D structure of lead compound within RBD D) lead compound docked in the binding groove of RBD E) vertical representation of lead compound interacting with RBM within RBD region F) 2D representation of interacting residues interacting with lead compound showing nature of interactions.

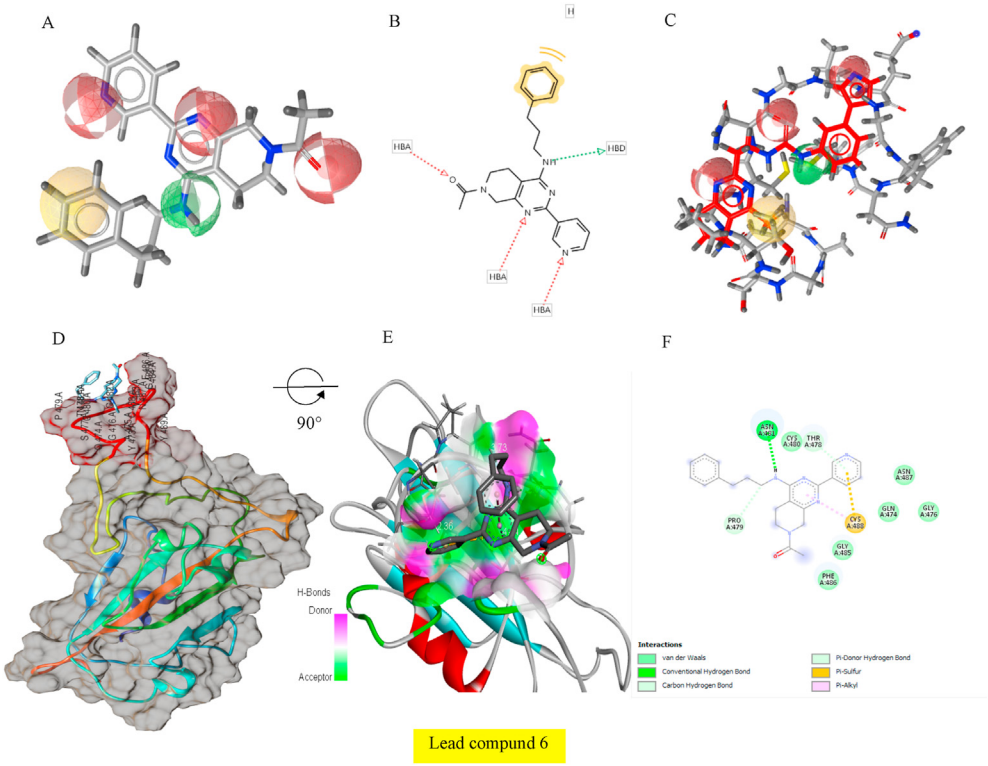

Figure 8. Virtually screened pharmacophore, lead molecule 6 and its interaction with RBD of spike glycoprotein. A) lead molecule 6 predicted in pharmacophore region B) 2D structure of lead compound with pharmacophore features C) 3D structure of lead compound within RBD D) lead compound docked in the binding groove of RBD E) vertical representation of lead compound interacting with RBM within RBD region F) 2D representation of interacting residues interacting with lead compound showing nature of interactions.

THR 478 with lead compound 5. GLN 474, ASN 487 interacts using halogen bond (Figure 6).

The docking score of lead compound 5 is -4.9. The interacting residues making Van der Waal's interaction are PHE 486, GLY 485, GLN 474, GLY 476, ASN 487, and CYS 480. THR 478 and PRO 479 interact with lead compound using pi donor Hydrogen bond. ASN 481 makes conventional hydrogen bond. CYS 488 make only pi-Sulphur bond with lead compound 5 (unlike in case of lead compound 3 where it makes two types of bonds) (Figure 7).

The lead compound 6 interacts with RBD with a docking score of -4.8. The interacting residues are PRO 479, GLY 485, ASN 487, GLN 474, CYS 480, PHE 486 makes Van der Waal's interaction with lead compound 6.

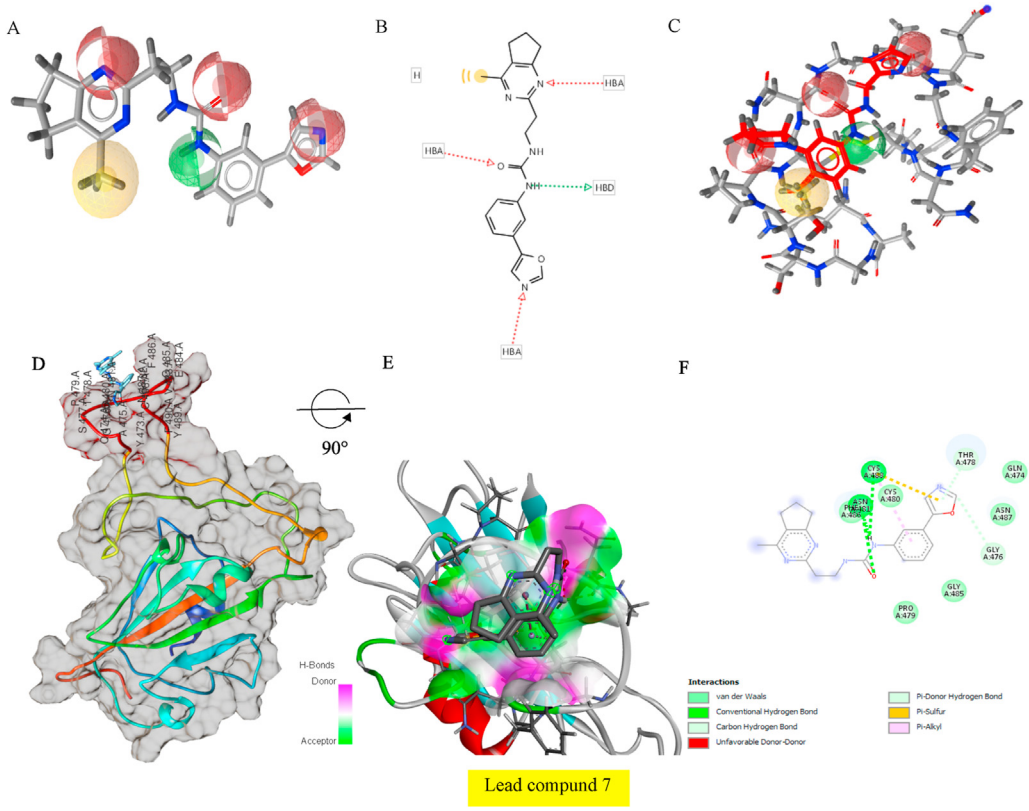

Figure 9. Virtually screened pharmacophore lead molecule 7 and its interaction with RBD of spike glycoprotein. A) lead molecule 7 predicted in pharmacophore region B) 2D structure of lead compound with pharmacophore features C) 3D structure of lead compound within RBD D) lead compound docked in the binding groove of RBD E) vertical representation of lead compound interacting with RBM within RBD region F) 2D representation of interacting residues interacting with lead compound showing nature of interactions.

THR 478 and GLY 476 makes pi donor hydrogen bond. Two conventional hydrogen bonds are predicted in docked complex of lead compound 6 and RBD that are made by CYS 488 and ASN 481 (Figure 8).

The lead compound 7 interacts with RBD with a docking score of -5.1. Only two residues are involved in making Van der Waal interaction that are THR 478, and VAL 483. GLY 482 residue makes C–H bond. Two conventional bonds are predicted that are made by ASN 487 and ASN 481. CYS 488 makes pi-Sulphur bond like it makes with lead compound 5. PHE 486 and GLY 485 make amide-pi stacked bond with lead compound 7. Lastly, CYS 480 makes alkyl bond (Figure 9).

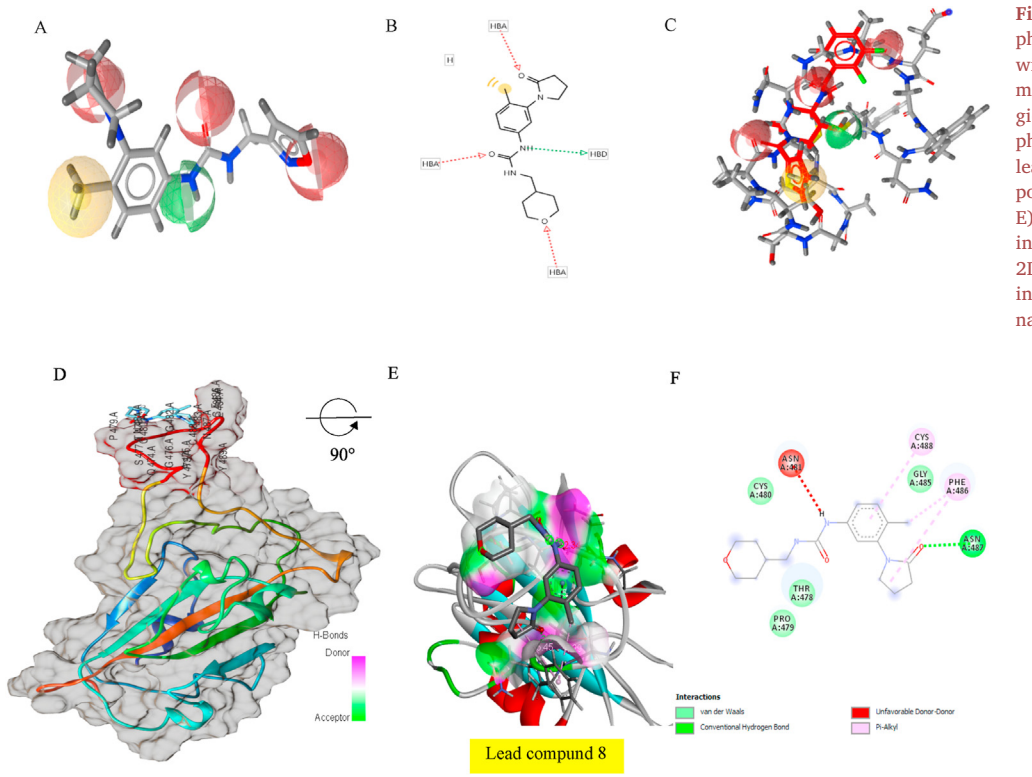

Figure 10. Virtually screened pharmacophore lead, molecule 8 and its interaction with RBD of spike glycoprotein. A) lead molecule 8 predicted in pharmacophore region B) 2D structure of lead compound with pharmacophore features C) 3D structure of lead compound within RBD D) lead compound docked in the binding groove of RBD E) vertical representation of lead compound interacting with RBM within RBD region F) 2D representation of interacting residues interacting with lead compound showing nature of interactions.

The lead compound 8 interacts with -5.1 docking score with RBD of S. The interacting residues making Van der Waal interaction are CYS 480, THR 478, PRO 479, GLY 485. CYS 488 and PHE 486 make pi alkyl bond. ASN 487 makes conventional hydrogen bond. However, ASN 481 in this interaction is unfavorable donor-donor (Figure 10).

The databases used in this study also contain FDA approved and experimental small ligands. The compounds predicted hereby interact with S region of SARS-CoV-2 with significant binding energy. The molecules are likewise predicted to be safe as per computational analysis, however, both aspects need experimental validation to be biologically validated. The molecules are reported in Cambridge and ZINC databases and can be synthesized. The safety profile of these lead compounds has also been assessed computationally (Groom et al., 2016; Irwin and Shoichet, 2005). Similar studies have been conducted by researchers in Brazil in which novel compounds against SARS-CoV-2 against main protease (da Silva Hage-Melim et al., 2020).

In past, the trend of novel drug prediction against viruses using virtual screening approach has also demonstrated successful application. The compounds reported hereby have good binding affinity with RBM of SARS-CoV-2 and their efficacy can be validated experimentally (Neves et al., 2018).

Literature studies reveal a number of SARS-CoV-2 inhibitors proposed computationally that target various regions of virus and protect against COVID-19. Peptide inhibitors using protease domain of ACE were reported to be potent against SARS-CoV-2 (Han and Král, 2020). Moreover, many computational studies focusing on drug repurposing have also been reported so far that interact with RNA dependent RNA polymerase of SARS-CoV-2 and prevent viral replication (Chakrabort et al., 2020). However, the compounds reported hereby are predicted to interact with RBM of S hence can prevent attachment to host cells.

The compounds reported herewith also comply with the standards of oral drugs and, if tested, experimentally can yield promising results.

4. Conclusion

All the lead compounds reported here in this study show significant interaction with active residues of RBM that have a role in attachment of S with both human receptors i.e., ACE2 and GRP78. The active residues involved in this interaction have been reported by Ibrahim et al. (2020) and used to design pharmacophore. The designed pharmacophore then, via virtual screening, shortlisted 8 drugs that can disrupt interaction of RBM of S with ACE2. Virtually screened drugs reported in this study interact with these 473–489 residues, RBM region of S, and can block viral entry by preventing viral attachment to host cells Moreover, the compounds virtually screened in this study are not under clinical and investigational trial against SARS-CoV-2 and experimental evaluation of lead compound can yield fruitful results opening gates of anti-viral drug discovery against SARS-CoV-2. These are preliminary findings and need experimental validation to check biological efficacy.

Declarations

Author contribution statement

Muhammad Shehroz, Tahreem Zaheer: Conceived and designed the experiments; Performed the experiments; Analyzed and interpreted the data; Wrote the paper.

Tanveer Hussain: Analyzed and interpreted the data; Contributed reagents, materials, analysis tools or data; Wrote the paper.

Funding statement

This research did not receive any specific grant from funding agencies in the public, commercial, or not-for-profit sectors.

Competing interest statement

The authors declare no conflict of interest.

Additional information

Supplementary content related to this article has been published online at https://doi.org/10.1016/j.heliyon.2020.e05278.

Acknowledgements

We want to acknowledge the administrative support provided by Virtual University of Pakistan to conduct this study. We would also like to thank reviewers for giving their valuable suggestions in improving the quality of manuscript.

References

Baez-Santos, Y.M., Mielech, A.M., Deng, X., Baker, S., Mesecar, A.D., 2014. Catalytic function and substrate specificity of the papain-like protease domain of nsp3 from the Middle East respiratory Syndrome coronavirus. J. Virol.
Belouzard, S., Millet, J.K., Licitra, B.N., Whittaker, G.R., 2012. Mechanisms of coronavirus cell entry mediated by the viral spike protein. Viruses 4 (6), 1011–1033.
Bogoch, I.I., Watts, A., Thomas-Bachli, A., Huber, C., Kraemer, M.U.G., Khan, K., 2020. Pneumonia of unknown aetiology in Wuhan, China: potential for international spread via commercial air travel. J. Trav. Med. 27 (2), taaa008.
Chakrabort, H., Paria, P., Gangopadhyay, A., Sayak, G., 2020. Drug Repurposing against SARS-CoV-2 RDRP - a Computational Quest against CoVID- 19.
da Silva Hage-Melim, L.I., Federico, L.B., de Oliveira, N.K.S., Francisco, V.C.C., Correa, L.C., de Lima, H.B., Gomes, S.Q., Barcelos, M.P., Francischini, I.A.G., others, 2020. Virtual screening, ADME/Tox predictions and the drug repurposing concept for future use of old drugs against the COVID-19. Life Sci. 117963.
Dong, L., Hu, S., Gao, J., 2020. Discovering drugs to treat coronavirus disease 2019 (COVID-19). Drug Dis. Ther. 14 (1), 58–60.
Groom, C.R., Bruno, I.J., Lightfoot, M.P., Ward, S.C., 2016. The Cambridge structural database. Acta Crystallogr. B: Struct. Sci. Crystal Eng. Mater. 72 (2), 171–179.
Han, Y., Král, P., 2020. Computational design of ACE2-based peptide inhibitors of SARS-CoV-2. ACS Nano 14 (4), 5143–5147.
Higueruelo, A.P., Jubb, H., Blundell, T.L., 2013. TIMBAL v2: update of a database holding small molecules modulating protein-protein interactions. Database.
Hoffmann, M., Kleine-Weber, H., Schroeder, S., Krüger, N., Herrler, T., Erichsen, S., Schiergens, T.S., Herrler, G., Wu, N.H., Nitsche, A., Müller, M.A., Drosten, C., Pöhlmann, S., 2020. SARS-CoV-2 cell entry depends on ACE2 and TMPRSS2 and is blocked by a clinically proven protease inhibitor. Cell.
Hui, D.S., I Azhar, E., Madani, T.A., Ntoumi, F., Kock, R., Dar, O., Ippolito, G., Mchugh, T.D., Memish, Z.A., Drosten, C., Zumla, A., Petersen, E., 2020. The continuing 2019-nCoV epidemic threat of novel coronaviruses to global health — the latest 2019 novel coronavirus outbreak in Wuhan, China. Int. J. Infect. Dis. 91, 264–266.
Ibrahim, I.M., Abdelmalek, D.H., Elfiky, A.A., 2019. GRP78: a cell's response to stress. Life Sci. 226, 156–163.
Ibrahim, I.M., Abdelmalek, D.H., Elshahat, M.E., Elfiky, A.A., 2020. COVID-19 spike-host cell receptor GRP78 binding site prediction. J. Infect.
Irwin, J.J., Shoichet, B.K., 2005. ZINC - a free database of commercially available compounds for virtual screening. J. Chem. Inf. Model. 45 (1), 177–182.
Kapetanovic, I.M., 2008. Computer-aided drug discovery and development (CADDD): in silico-chemico-biological approach. Chem. Biol. Interact. 171 (2), 165–176.
Kim, Y., Lillo, A.M., Steiniger, S.C.J., Liu, Y., Ballatore, C., Anichini, A., Mortarini, R., Kaufmann, G.F., Zhou, B., Felding-Habermann, B., Janda, K.D., 2006. Targeting heat shock proteins on cancer cells: selection, characterization, and cell-penetrating properties of a peptidic GRP78 ligand. Biochemistry 45 (31), 9434–9444.
Kumar, S., Stecher, G., Li, M., Knyaz, C., Tamura, K., 2018. MEGA X: molecular evolutionary genetics analysis across computing platforms. Mol. Biol. Evol. 35 (6), 1547–1549.
Lee, A.S., 2005. The ER chaperone and signaling regulator GRP78/BiP as a monitor of endoplasmic reticulum stress. Methods 35 (4), 373–381.
Letunic, I., Bork, P., 2019. Interactive Tree of Life (iTOL) v4: recent updates and new developments. Nucleic Acids Res. 47 (W1), W256–W259.
Li, F., 2016. Structure, function, and evolution of coronavirus spike proteins. Ann. Rev. Virol. 3, 237–261.
Li, F., Li, W., Farzan, M., Harrison, S.C., 2005a. Structural biology: structure of SARS coronavirus spike receptor-binding domain complexed with receptor. Science 309 (5742), 1864–1868.
Li, J., Lee, A., 2006. Stress induction of GRP78/BiP and its role in cancer. Curr. Mol. Med. 6 (1), 45–54.
Li, W., Shi, Z., Yu, M., Ren, W., Smith, C., Epstein, J.H., Wang, H., Crameri, G., Hu, Z., Zhang, H., Zhang, J., McEachern, J., Field, H., Daszak, P., Eaton, B.T., Zhang, S., Wang, L.F., 2005b. Bats are natural reservoirs of SARS-like coronaviruses. Science 310 (5748), 676–679.
Lipinski, C.A., 2004. Lead- and drug-like compounds: the rule-of-five revolution. Drug Discov. Today Technol. 1 (4), 337–341.

Lyne, P.D., 2002. Structure-based virtual screening: an overview. Drug Discov. Today 7 (20), 1047–1055.
Munster, V.J., Koopmans, M., van Doremalen, N., van Riel, D., de Wit, E., 2020. A novel coronavirus emerging in China - key questions for impact assessment. N. Engl. J. Med. 382 (8), 692–694.
Neves, B.J., Braga, R.C., Melo-Filho, C.C., Moreira-Filho, J.T., Muratov, E.N., Andrade, C.H., 2018. QSAR-based virtual screening: advances and applications in drug discovery. Front. Pharmacol. 9, 1275.
Organization, W.H., 2019. Clinical Management of Severe Acute Respiratory Infection when Middle East Respiratory Syndrome Coronavirus (MERS-CoV) Infection Is Suspected: Interim Guidance. World Health Organization.
Paules, C.I., Marston, H.D., Fauci, A.S., 2020. Coronavirus infections-more than just the common cold. JAMA - J. Am. Med. Assoc. 323 (8), 707–708.
Pettersen, E.F., Goddard, T.D., Huang, C.C., Couch, G.S., Greenblatt, D.M., Meng, E.C., Ferrin, T.E., 2004. UCSF Chimera - a visualization system for exploratory research and analysis. J. Comput. Chem. 25 (13), 1605–1612.
Prajapat, M., Sarma, P., Shekhar, N., Avti, P., Sinha, S., Kaur, H., Kumar, S., Bhattacharyya, A., Kumar, H., Bansal, S., Medhi, B., 2020. Drug targets for corona virus: a systematic review. Indian J. Pharmacol. 52 (1), 56.
Quinones, Q.J., de Ridder, G.G., Pizzo, S.V., 2008. GRP78: a chaperone with diverse roles beyond the endoplasmic reticulum. Histol. Histopathol.
Rao, R.V., Ellerby, H.M., Bredesen, D.E., 2004. Coupling endoplasmic reticulum stress to the cell death program. Cell Death Differ. 11 (4), 372–380.
Shang, J., Ye, G., Shi, K., Wan, Y., Luo, C., Aihara, H., Geng, Q., Auerbach, A., Li, F., 2020. Structural basis of receptor recognition by SARS-CoV-2. Nature 581 (7807), 221–224.
Shen, J., Chen, X., Hendershot, L., Prywes, R., 2002. ER stress regulation of ATF6 localization by dissociation of BiP/GRP78 binding and unmasking of golgi localization signals. Dev. Cell 3 (1), 99–111.
Stahura, F., Bajorath, J., 2012. Virtual screening methods that complement HTS. Comb. Chem. High Throughput Screen. 7 (4), 259–269.
Sudha, K.N., Shakira, M., Prasanthi, P., Sarika, N., Kumar, C.N., Babu, P.A., 2008. Virtual screening for novel COX-2 inhibitors using the ZINC database. Bioinformation 2 (8), 325.
Tang, X., Wu, C., Li, X., Song, Y., Yao, X., Wu, X., Duan, Y., Zhang, H., Wang, Y., Qian, Z., Cui, J., Lu, J., 2020. On the origin and continuing evolution of SARS-CoV-2. Nat. Sci. Rev.
Trott, O., Olson, A.J., 2009. AutoDock Vina: improving the speed and accuracy of docking with a new scoring function, efficient optimization, and multithreading. J. Comput. Chem. 31 (2), 455–461.
Udwadia, Z.F., Raju, R.S., 2020. How to protect the protectors: 10 lessons to learn for doctors fighting the COVID-19 Coronavirus. Med. J. Armed Forces India.
Visualizer, D.S., 2005. v4. 0.100. 13345. Accelrys Software Inc.
Walls, A.C., Park, Y.J., Tortorici, M.A., Wall, A., McGuire, A.T., Veesler, D., 2020. Structure, function, and antigenicity of the SARS-CoV-2 spike glycoprotein. Cell.
Wang, Z., Sun, H., Yao, X., Li, D., Xu, L., Li, Y., Tian, S., Hou, T., 2016. Comprehensive evaluation of ten docking programs on a diverse set of protein-ligand complexes: the prediction accuracy of sampling power and scoring power. Phys. Chem. Chem. Phys. 18 (18), 12964–12975.
WHO, 2018. Emergencies Preparedness , Response. WHO.
Widagdo, W., Okba, N.M.A., Stalin Raj, V., Haagmans, B.L., 2017. MERS-coronavirus: from discovery to intervention. One Health 3, 11–16.
Wishart, D.S., 2012. DrugBank. Princ. Pharmacog. Pharmacogenom.
Wolber, G., Langer, T., 2005. LigandScout: 3-D pharmacophores derived from protein-bound ligands and their use as virtual screening filters. J. Chem. Inf. Model. 45 (1), 160–169.
Yang, J., Zhang, Y., 2015. Protein structure and function prediction using I-tasser. Curr. Protocol. Bioinformat. 52 (1), 5–8.
Yang, S.Y., 2010. Pharmacophore modeling and applications in drug discovery: challenges and recent advances. Drug Discov. Today 15 (11-12), 444–450.
Zhao, S., Lin, Q., Ran, J., Musa, S.S., Yang, G., Wang, W., Lou, Y., Gao, D., Yang, L., He, D., Wang, M.H., 2020. Preliminary estimation of the basic reproduction number of novel coronavirus (2019-nCoV) in China, from 2019 to 2020: a data-driven analysis in the early phase of the outbreak. Int. J. Infect. Dis. 92, 214–217.